

Navier-Stokes equation describes the movement of a special superfluid medium

Valeriy I. Sbitnev*

*St. Petersburg B. P. Konstantinov Nuclear Physics Institute,
NRC Kurchatov Institute, Gatchina, Leningrad district, 188350, Russia;
Department of Electrical Engineering and Computer Sciences,
University of California, Berkeley, Berkeley, CA 94720, USA*

(Dated: December 3, 2024)

The Navier-Stokes equation contains two terms which have been subjected to slight modification: (a) the viscosity term depends of time (the viscosity in average on time is zero, but its variance is nonzero); (b) the pressure gradient contains an added term describing the entropy gradient multiplied by the pressure. Owing to these modifications, the Navier-Stokes equation can be reduced to the Schrödinger equation describing behavior of a particle into the vacuum, where the vacuum is a superfluid medium. Vortex structures arising in this medium show infinitely long life owing to zero average viscosity. The nonzero variance describes exchange of the vortex energy with zero-point energy of the vacuum. Radius of the vortex trembles around some average value. This observation sheds the light to the Zitterbewegung phenomenon. The vortex has a non-zero core where the vortex velocity vanishes. Its organization is discussed with the point of view of the Calabi-Yau manifold.

Keywords: Navier-Stokes; Schrödinger; zero-point fluctuations; superfluid vacuum; vortex; Calabi-Yau manifold; Bohmian trajectory; interference

I. INTRODUCTION

For about 100 years of the study of quantum-mechanical phenomena, the Schrödinger equation has proved to be a reliable equation. Its solutions give good agreement with experiments. The solution of this equation is represented through a complex-valued function $\psi(\vec{r}, t)$, called the wave function. Observable variables, A and others, are expressed through scalar product $\langle \psi | A | \psi \rangle$, which represents the statistical expectation of this variable. From the very beginning of the birth of the quantum mechanics as a science, the question arose what can be the physical meaning of the wave function?

Without going into details of various interpretations of the quantum mechanics [17], we note that immediately behind the famous article of Erwin Schrödinger published in 1926 [40], an article of Erwin Madelung appeared in the same year. This article was entitled "Quantum theory in hydrodynamical form" [28]. Madelung compares the wave function represented in the polar form $\psi = R \exp\{iS/\hbar\}$ with a peculiar fluid, which flows according to laws described in this article. The laws follow from the quite famous

equations. The first equation is the Hamilton-Jacobi equation loaded by the extra term having a view

$$Q = -\frac{\hbar^2}{2m} \frac{\nabla^2 R}{R}. \quad (1)$$

And the second equation is the continuity equation for the probability density $\rho = R^2$. Here R is the probability amplitude, \hbar is the reduced Planck constant, and m is the mass of a particle to be interesting. Since Madelung's article was published in a German magazine, his ideas remained for a long time outside the focus of attention of the scientific community.

Similar computations were made by David Bohm in 1952 and published in the journal Physical Review [5, 6]. Immediately following these publications, David Bohm and Jean-Pierre Vigier have published an article concerning a causal interpretation of quantum mechanics, in which a set of fields is equivalent in many ways to a conserved fluid [7]. Interest to searching analogies between quantum mechanical phenomena and hydrodynamical ones stays always heightened [8, 10, 18, 20, 23, 46].

After Bohm's publications [5, 6], the term (1) is named the quantum potential and the computations given in these articles are represented further as the Bohmian mechanics [3, 27]. Bohm's version of quantum mechanics was practically a

*Electronic address: valery.sbitnev@gmail.com

mathematical interpretation of the de Broglie pilot-wave theory. According to this theory, there is a wave accompanying the particle from its birth on a source until it will be registered on a detector [11]. The particle is represented as a singularity moving along the optimal trajectory. The latter is formed due to the interference of the pilot-wave accompanying particle.

Surprisingly, the confirmation of the correctness of the de Broglie theory came from an unexpected side [9, 14, 33]: at studying the motion of drops on the oil surface subjected to transverse oscillations of very small amplitude, scientists observed interference of the surface waves induced by the droplet bouncing. Observations show that, when the droplet bounces off from the surface, the waves caused by the impact of the droplet, spread far from the touch of the droplets, creating constructive and destructive interference of the surface waves. So, when the droplet touches down to the surface again it faces with such an inclination of the surface from which it bounces off to a right direction (like a tennis ball, for instance, bounces off the racket in a direction desired for player). When passing the droplets through a barrier, having two slits, interference fringes are observed in the far-field zone after accumulation of a sufficient statistics [9].

Let us imagine that the sub-critical Faraday waves induced on the fluid surface simulate, in some way, the zero-point fluctuations of the physical vacuum. In other words, the physical vacuum represents itself as a special fluid - the superfluid one [13, 44]. For that reason we may apply the Navier-Stokes equation for description of its state [38, 39], where the viscosity in the first approximation is zero.

Two equations which have a crucial significance here are the Navier-Stokes equation

$$\begin{aligned} & \rho_M \left(\frac{\partial \vec{v}}{\partial t} + (\vec{v} \cdot \nabla) \vec{v} \right) \\ &= \frac{\vec{F}}{\Delta V} - \rho_M \nabla \left(\frac{P}{\rho_M} \right) + \mu(t) \nabla^2 \vec{v}. \quad (2) \end{aligned}$$

and the continuity equation

$$\frac{\partial \rho_M}{\partial t} + (\vec{v} \cdot \nabla) \rho_M = 0. \quad (3)$$

Here $\rho_M = M/\Delta V$ is a mass density of the fluid in the volume ΔV that is under consideration, \vec{v} is a flow velocity, and $\vec{F}/\Delta V$ is an external force per the volume ΔV . There are internal forces that are represented by pressure gradients within the fluid and dissipative forces arising due to the fluid viscosity. They are represented by the last two terms in Eq. (2). The following modifications of these terms are important in this article: (a) the dynamic viscosity μ , in average equal to zero, fluctuates in time; (b) the pressure gradient is subjected to a slight modification, namely $\nabla P \rightarrow \rho_M \nabla(P/\rho_M) = \nabla P - P \nabla \ln(\rho_M)$. This modification will be important for us when we shall begin to derive the Schrödinger equation.

The article is organized as follows. Sect. II deals with consideration of the Navier-Stokes equation in the light of derivation of the Schrödinger equation. A main point here lies in finding the quantum potential (1). Sect. III discusses the Bohmian trajectories and the uncertainty principle relating to them. In Sect. IV we examine the Helmholtz vortices with the viscosity oscillating in time. The spherical vortices, vortex balls, are compact versions of the toroidal vortices which are considered as possible particle models having spins. In Sect. V, the concluding section, we consider different interpretations of quantum mechanics in the light of these findings. Significance of the superfluid vacuum medium for existence of the particles with spins is emphasized.

II. DERIVATION OF THE SCHRÖDINGER EQUATION

First let us rewrite the mass density ρ_M according to the following presentation

$$\rho_M = \frac{M}{\Delta V} = \frac{mN}{\Delta V} = m\rho. \quad (4)$$

Here the mass M is a product of an elementary mass m by the number of these masses, N , filling the volume ΔV . We believe the sub-particles

with the mass m are identical [21]. Then the mass density ρ_M is defined as a product of the elementary mass m by the density of sub-particles $\rho = N/\Delta V$. Also we believe that the sub-particles perform the Brownian motions [32] in the fluid medium. The diffusion coefficient of the Brownian motion is follows

$$D = \frac{\hbar}{2m}. \quad (5)$$

The Brownian motion of sub-particles represents an important essence in Nelson's work [32] determining state of aether wherein all quantum events occur. In our case, this medium is a physical vacuum populated by enormous numbers of particle-antiparticle pairs.

A. Where does the quantum potential come from?

We begin with a modified pressure gradient

$$\rho_M \nabla \left(\frac{P}{\rho_M} \right) = \rho \nabla \left(\frac{P}{\rho} \right) = \nabla P - P \nabla \ln(\rho). \quad (6)$$

The first term, the pressure gradient ∇P , is represented in the usual Navier-Stokes equation [24, 25]. Whereas, the second term, $P \nabla \ln(\rho)$, is an extra term describing changing the logarithm of the density distribution ρ on increment of length multiplied by P . It may mean that change of the pressure is induced by change of the entropy per length, or else by change of the information flow [26, 35] per length.

First, let us represent the pressure P as consisting of the sum of the two pressures P_1 and P_2 . As for the pressure P_1 we begin with the Fick's law [16]. The law says that the diffusion flux, \vec{J} , is proportional to the negative value of the density gradient $\vec{J} = -D \nabla \rho_M$. Next, since the term $D \nabla \vec{J}$ has dimension of the pressure, we define:

$$P_1 = D \nabla \vec{J} = -\frac{\hbar^2}{4m^2} \nabla^2 \rho_M. \quad (7)$$

Here we are replacing the diffusion coefficient D through its expression shown in Eq. (5). Observe that the kinetic energy of the diffusion flux is $(m/2)(\vec{J}/\rho_M)^2$. It means that there exists one

more pressure as the average momentum transfer per unit area per unit time:

$$P_2 = \frac{\rho_M}{2} \left(\frac{\vec{J}}{\rho_M} \right)^2 = \frac{\hbar^2}{8m^2} \frac{(\nabla \rho_M)^2}{\rho_M}. \quad (8)$$

Now we can see that sum of the two pressures, $P_1 + P_2$, divided by ρ (we remark that $\rho_M = m\rho$, see Eq. (4)) reduces to the quantum potential

$$Q = \frac{P_2 + P_1}{\rho} = \frac{\hbar^2}{8m} \left(\frac{\nabla \rho}{\rho} \right)^2 - \frac{\hbar^2}{4m} \frac{\nabla^2 \rho}{\rho}. \quad (9)$$

Now the Navier-Stokes equation (2) divided by ρ takes a view

$$\begin{aligned} m \left(\frac{\partial \vec{v}}{\partial t} + (\vec{v} \cdot \nabla) \vec{v} \right) \\ = \frac{\vec{F}}{N} - \nabla Q + \nu(t) \nabla^2 m \vec{v}. \end{aligned} \quad (10)$$

Here \vec{F}/N is the external force per the sub-particle. The kinetic viscosity $\nu(t) = \mu(t)/\rho_M$ has the dimension [length²/time] and fluctuates alternately about zero. Let its amplitude be equal to the diffusion coefficient (5).

B. Irrotational and solenoidal vector fields

The fundamental theorem of vector calculus states that any vector field can be expressed as the sum of an irrotational and a solenoidal field. The current velocity \vec{v} can be represented consisting of two components – irrotational and solenoidal [24]:

$$\vec{v} = \vec{v}_S + \vec{v}_R, \quad (11)$$

where subscripts S and R point to existence of scalar and vector (rotational) potentials underlying emergence of these velocities. These velocities relate to vortex-free and vortex motions of the fluid medium, respectively. Scalar and vector fields underlie of manifestation of these two types of the velocities. They satisfy the following equations

$$\begin{cases} (\nabla \cdot \vec{v}_S) \neq 0, & [\nabla \times \vec{v}_S] = 0, \\ (\nabla \cdot \vec{v}_R) = 0, & [\nabla \times \vec{v}_R] = \vec{\omega}. \end{cases} \quad (12)$$

Also we shall write down the term $(\vec{v} \cdot \nabla) \vec{v}$ in Eq. (10) in detail

$$(\vec{v} \cdot \nabla) \vec{v} = \nabla v^2/2 + [\vec{\omega} \times \vec{v}]. \quad (13)$$

Here $\vec{\omega} = [\nabla \times \vec{v}]$ is the vorticity.

Let us now designate the scalar field by a scalar function S , having name the action. Then the irrotational velocity \vec{v}_s of the sub-particle is defined as $\nabla S/m$. Next, the momentum and the kinetic energy of the sub-particle are as follows

$$\begin{cases} \vec{p} = m\vec{v} = \nabla S + m\vec{v}_R, \\ m\frac{v^2}{2} = \frac{1}{2m}(\nabla S)^2 + m\frac{v_R^2}{2}. \end{cases} \quad (14)$$

As seen in the bottom line, the kinetic energy of the fluid motion is equal to sum of the kinetic energies of irrotational and solenoidal motions.

Now taking into account the expression (13) we may rewrite the Navier-Stokes equation (10)

in the more detailed form

$$\begin{aligned} & \frac{\partial}{\partial t}(\nabla S + m\vec{v}_R) \\ & + \left\{ \frac{1}{2m} \nabla \left((\nabla S)^2 + m^2 v_R^2 \right) + m[\vec{\omega} \times \vec{v}_R] \right\} \\ & = -\nabla U - \nabla Q + \nu(t) \nabla^2 (\nabla S + m\vec{v}_R). \end{aligned} \quad (15)$$

Here we take into account that the external force in the Navier-Stokes equation (10) is conservative, i.e., $\vec{F}/N = -\nabla U$, where U is the potential energy relating to the single sub-particle. The terms ∇U and ∇Q are gradients of the potential energy and of the quantum potential, respectively. The third term in the second line describes the viscosity of the medium. As was said above the viscosity coefficient in the average is equal to zero.

Let us rewrite Eq. (15) by regrouping the terms

$$\nabla \left(\underbrace{\frac{\partial}{\partial t} S + \frac{1}{2m}(\nabla S)^2 + \frac{m}{2}v_R^2 + U + Q - \nu(t)\nabla^2 S}_{f_1(\vec{r},t)} \right) = \underbrace{-m\frac{\partial}{\partial t}\vec{v}_R - m[\vec{\omega} \times \vec{v}] + \nu(t)m\nabla^2\vec{v}_R}_{\vec{f}_2(\vec{r},t)}. \quad (16)$$

Here the curly brackets single out two qualitatively different functions, scalar-valued function $f_1(\vec{r},t)$ and vector-valued function $\vec{f}_2(\vec{r},t)$. Depending on application of the ∇ -operator, either as inner product of this operator or the cross product, we may extract either the left side or the right side of this expression.

Let us multiply Eq. (16) by the curl. We get:

$$\nabla \times \nabla f_1(\vec{r},t) = 0. \quad (17)$$

It means that the function $f_1(\vec{r},t)$ can be any scalar function of \vec{r} and t , like the potential U . By supposing that its dependence from \vec{r} and t is extremely small, we take $f_1(\vec{r},t) = C$. Here C is an arbitrary constant. As a result of this computation, we come to the following modified Hamilton-Jacobi equation

$$\frac{\partial}{\partial t} S + \frac{1}{2m}(\nabla S)^2 + \frac{m}{2}v_R^2 + U + Q = C. \quad (18)$$

The modification of this equation is due to the presence of the quantum potential Q , see Eq. (9).

We believe that the viscosity $\nu(t)$ fluctuates about zero much more frequent, than characteristic time of displacements of the sub-particles. For that reason, we omit in Eq. (18) the terms containing $\nu(t)$ by supposing in the first approximation, that the medium is absolutely superfluid. In other words, we assume that there are no energy sources and sinks.

The second equation in addition to the modified Hamilton-Jacobi equation (18) is the continuity equation

$$\frac{\partial \rho}{\partial t} + (\vec{v} \cdot \nabla) \rho = 0 \quad (19)$$

rewritten from Eq. (3) in accordance with (4). Eqs. (18) and (19) are seen to be crucial equations in the Bohmian mechanics [3, 5, 6].

These both equations, Eqs. (18) and (19), can be easily extracted [3, 35] from the following Schrödinger equation

$$i\hbar \frac{\partial \Psi}{\partial t} = \frac{1}{2m}(-i\hbar \nabla + m\vec{v}_R)^2 \Psi + U(\vec{r})\Psi - C\Psi. \quad (20)$$

The kinetic momentum operator $(-i\hbar \nabla + m\vec{v}_R)$ contains the term $m\vec{v}_R$ describing a contribution of the vortex motion. This term is analogous to the vector potential [4, 31] multiplied by the ratio of the charge to the light speed, which appears in quantum electrodynamics.

By substituting into Eq (20) the wave function Ψ represented in a polar form

$$\Psi = \sqrt{\rho} \exp\{iS/\hbar\} \quad (21)$$

and separating on real and imaginary parts we come to Eqs. (18) and (19). So, the Navier-Stokes equation (2), with slightly expanded the pressure gradient term ∇P , can be reduced to the Schrödinger equation. Presence of the extra term $P\nabla \ln(\rho)$, as was shown earlier, provides the right introduction of the quantum potential.

III. BOHMIAN TRAJECTORIES AND THE UNCERTAINTY PRINCIPLE

The Shrödinger wave equation can be resolved by heuristic writing of a solution through using the Huygens' principle. In its mathematical presentation the solution is given by the Feynman path integral [15, 29]:

$$\Psi(\vec{r}, t) = \int K(\vec{r}, \vec{\xi}; t) \Psi(\vec{\xi}, 0) d\vec{\xi}. \quad (22)$$

The propagator $K(\vec{r}, \vec{\xi}; t)$ contains information on a physical space loaded by a physical equipment, such as sources, detectors, collimators, gratings, etc. This physical scene is simulated by the potential $U(\vec{r})$ presented in the Schrödinger equation and by the boundary conditions superposed on it. So, a solution of the Schrödinger equation can be achieved by applying the Feynman path integral technique [12, 15].

By applying this technique for describing the wave propagation through a lattice consisting of

N slits we get the solution [36]

$$|\Psi(x, z)\rangle = \frac{1}{N\sqrt{1 + i\frac{\lambda z}{2\pi b^2}}} \cdot \sum_{n=0}^{N-1} \left\{ -\frac{\left(x - \left(n - \frac{N-1}{2}\right)d\right)^2}{2b^2 \left(1 + i\frac{\lambda z}{2\pi b^2}\right)} \right\}. \quad (23)$$

Here $i = \sqrt{-1}$ is imaginary unit, λ is the de Broglie wavelength, b is the slit width, and d is the distance between slits.

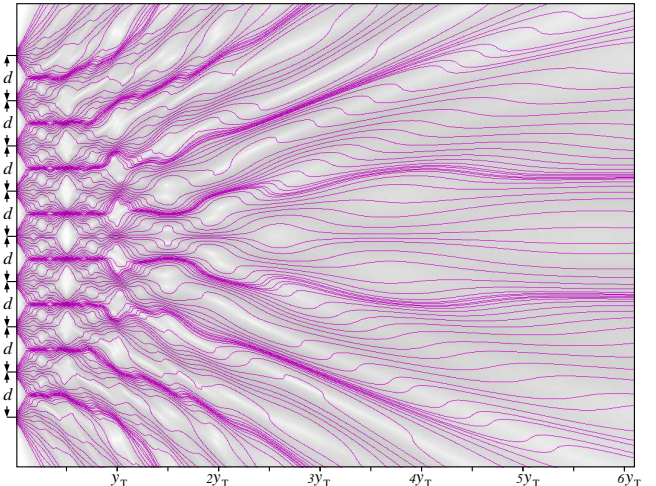


FIG. 1: Interference pattern of the coherent flow of fullerene molecules with de Broglie wavelength $\lambda = 5$ pm within a zone $z \leq 6z_T$ from the grating containing 9 slits. The scale along the axis z is given in the Talbot lengths, $z_T = 2d^2/\lambda = 0.025$ m, where $d = 250$ nm. Black curves against the grey background represent the Bohmian trajectories.

The density distribution function is a scalar product of the wave function $|\Psi(x, z)\rangle$:

$$p(x, z) = \langle \Psi(x, z) | \Psi(x, z) \rangle. \quad (24)$$

It is shown in gray scale in Fig. 1. These calculations show interference of the coherent flow of fullerene molecules [37] from the grating containing 9 slits. The fullerene molecules have the de Broglie wavelength $\lambda = 5$ pm what corresponds to the current velocity of the molecules about 100 m/s [22]. Parameters of the grating are as follows: width of the slit $b = 5 \cdot 10^3 \lambda = 25$ nm, distance between the slits $d = 5 \cdot 10^4 = 250$ nm.

Black curves drawn against the grey background in Fig. 1 are the Bohmian trajectories.

Their computations can be found, for instance, in [3]. Here we shall compute these trajectories by adopting the velocity operator that have the form $\hat{v} = -i\hbar/m\nabla$. For the computation we use the wave function $|\Psi\rangle$ represented in the polar form (21) with the amplitude density R instead of the probability density $\rho = R^2$. The computations give:

$$\begin{aligned}\vec{U} &= \frac{1}{R^2} \langle \Psi \left| -i\frac{\hbar}{m} \nabla \right| \Psi \rangle \\ &= \frac{1}{m} \nabla S - i\frac{\hbar}{m} \frac{\nabla R}{R}.\end{aligned}\quad (25)$$

Hereinafter $R^2 = \langle \Psi | \Psi \rangle$.

Real part in this expression is the current velocity of the particle

$$\vec{v} = \text{Re } \vec{U} = \frac{1}{m} \nabla S. \quad (26)$$

Whereas imaginary part

$$\vec{u} = -\text{Im } \vec{U} = \frac{\hbar}{m} \frac{\nabla R}{R}. \quad (27)$$

represents the osmotic velocity [32], which has a deep relation with the quantum potential (1).

Position of the particle in each current time starting from any slit up to the detector can be calculated by the following increment formula

$$\vec{r}(t + \delta t) = \vec{r}(t) + \vec{v}(t) \delta t. \quad (28)$$

Here t is the time that starts from $t = 0$ on a source within the slit and δt is an arbitrarily small increment of time. Some calculated trajectories, the Bohmian trajectories [5, 6], are shown in Fig. 1 as black wavy lines.

A. The uncertainty principle

As say, the calculations of (26) and (28) executable simultaneously are incompatible because of the uncertainty principle. For that reason we need also to check divergence of the above computations [37]. This computation gives

$$\begin{aligned}\text{Var}(\vec{U}) &= \frac{1}{R^2} \langle \Psi \left| \left(-i\frac{\hbar}{m} \nabla - \vec{U} \right)^2 \right| \Psi \rangle \\ &= \frac{1}{R^2} \langle \Psi \left| i\frac{\hbar}{m} \nabla \vec{U} + \underbrace{i\frac{\hbar}{m} \vec{U} \nabla}_{(a)} + \vec{U}^2 - \frac{\hbar^2}{m^2} \Delta \right| \Psi \rangle.\end{aligned}\quad (29)$$

The terms over curly bracket (a) kill each other since the operator $i(\hbar/m)\nabla$ reproduces $-\vec{U}$, see Eq. (25). It is reasonable in the perspective to multiply the above expression by $m/2$:

$$\frac{m}{2} \text{Var}(\vec{U}) = -\frac{1}{R^2} \langle \Psi \left| \frac{\hbar^2}{2m} \Delta \right| \Psi \rangle + i\frac{\hbar}{2} \nabla \vec{U} \quad (30)$$

So, this expression has a dimensionality of energy. After a number of computations we get the following result [37]:

$$\begin{aligned}\frac{m}{2} \text{Var}(\vec{U}) &= \underbrace{\frac{1}{2m} (\nabla S)^2}_{(b)} - \frac{\hbar^2}{2m} \left[\frac{\nabla R}{R} \right]^2 \\ &\quad - i\frac{\hbar}{m} \frac{(\nabla S \cdot \nabla R)}{R} \\ &= \frac{m}{2} \left(\frac{1}{m} \nabla S - i\frac{\hbar}{m} \frac{\nabla R}{R} \right)^2 = \frac{m}{2} \mathcal{U}^2.\end{aligned}\quad (31)$$

From here we see that the term $(m/2)\text{Var}(\vec{U})$ contains both the kinetic energy of the particle $(m^2/2)(\nabla S)^2$ and the energy of the osmotic motion $(\hbar^2/2m)(\nabla R/R)^2$. The generalization of the kinetic energy by expanding it in the imaginary area belongs the complexified Lagrangian mechanics [35].

Further we shall consider only real part of the expression covered by curly bracket (b):

$$\frac{m}{2} \text{Re Var}(\vec{U}) = \frac{1}{2m} (\nabla S)^2 - \frac{\hbar}{2} \omega_Q \geq 0. \quad (32)$$

The first term here is the kinetic energy, E , of the particle. And the term

$$\omega_Q = \frac{\hbar}{m} \left[\frac{\nabla R}{R} \right]^2, \quad (33)$$

stemming from the quantum potential, is a frequency of perturbation of the fluid medium named the physical vacuum. This perturbation is induced by the particle moving through the vacuum.

Let two particles have nearest trajectories. For the first particle we have $E_1 - \hbar\omega_{Q,1}$ and for the second particle $E_2 - \hbar\omega_{Q,2}$. Subtracting one from other we have

$$\delta E - \frac{\hbar}{2} \delta\omega_Q \geq 0. \quad (34)$$

Two particles moving along the trajectories placed near each other induce perturbations the kinetic energies during the time $\delta t = 1/\delta\omega_Q$. From here we have

$$\delta E \delta t \geq \frac{\hbar}{2}. \quad (35)$$

These perturbations play a role of measurements of some attributes of the particles.

Let us return now to Eq. (28) and rewrite it in the following view

$$\delta \vec{r}(t) = \vec{v}_1(t) \delta t \geq \vec{v}_1(t) \hbar / \delta E. \quad (36)$$

The initial Bohmian trajectory is marked here by subscript 1. Here $\delta E = m(v_2^2 - v_1^2)/2 \approx m\vec{v}_1 \delta \vec{v}$, and we calculated $v_2^2 = (\vec{v}_1 + \delta \vec{v})^2 \approx v_1^2 + 2\vec{v}_1 \delta \vec{v}$. Substituting computations of δE into Eq. (36) and taking into account that $m\delta \vec{v} = \delta \vec{p}$ we obtain finally

$$\delta \vec{p} \delta \vec{r} \geq \frac{\hbar}{2}. \quad (37)$$

The uncertainty principle is the fundamental principle of measurements. In this respect the Bohmian trajectories are really "hidden entities" with the point of view of this principle. Attempt to measure attributes of the particle moving along the Bohmian trajectory faces with the uncertainty of position the particle on the trajectory and its velocity along. A very small quantity of molecules or atoms in an experimental device can represent by themselves "sources of unpredictable measurements". It leads to deterioration of the visibility of the interference fringes [37].

IV. VORTEX DYNAMICS

Let us return to Eq. (16). From the right side the vector term $\vec{f}_2(\vec{r}, t)$ fell out of our consideration. By multiplying this equation by curl we got Eq. (17) Consequently $\nabla \times \vec{f}_2(\vec{r}, t) = 0$ and we find the equation for the vorticity

$$\frac{\partial \vec{\omega}}{\partial t} + (\vec{\omega} \cdot \nabla) \vec{v} = \nu(t) \nabla^2 \vec{\omega}. \quad (38)$$

The rightmost term describes dissipation of the energy stored in the vortex. As a result, the vortex with the lapse of time should disappear. By

omitting this rightmost term ($\nu = 0$) we open the action of the Helmholtz theorem: (i) if fluid particles form, in any moment of the time, a vortex line, then the same particles support the vortex line both in the past and in the future; (ii) ensemble of the vortex lines traced through a closed contour forms a vortex tube; (iii) intensity of the vortex tube is constant along its length and does not change in time. The vortex tube (a) either goes to infinity by both endings; (b) or these endings lean on boundary walls containing the fluid; (c) or these endings are locked to each on other forming a vortex ring.

Assuming that the fluid is a physical vacuum, which meets the requirements specified earlier, we must say that the viscosity vanishes. In that case, the vorticity $\vec{\omega}$ is concentrated in the center of the vortex, i.e., in the point. Its mathematical representation is δ -function. This singularity can be a source of possible divergences of computations in further.

We shall not remove the viscosity. Instead of that, we hypothesize that even if there is arbitrary small viscosity, because of the zero-point oscillations in the vacuum, the vortex does not disappear completely. The vortex can be a long-lived object. The foundation for that hypothesis is the observation (performed by French scientific team [9, 14, 33]) of behavior of the droplets moving on the oil surface, on which the waves Faraday exist. Here an important moment is that the Faraday waves are supported slightly below the super-critical threshold. Due to this trick the droplets can live arbitrary long, before they disappear in the oil. The Faraday waves that are supported in the vicinity of the super-critical threshold may play a role analogous to the zero-point oscillations of the vacuum.

Here we shall consider a simple model of such a picture. Let us look on the vortex tube in its cross-section which is oriented along the axis z and its center is placed in the coordinate origin of the plane (x, y) . Eq. (38), written down in the cross-section of the vortex, is as follows

$$\frac{\partial \omega}{\partial t} = \nu(t) \left(\frac{\partial^2 \omega}{\partial r^2} + \frac{1}{r} \frac{\partial \omega}{\partial r} \right). \quad (39)$$

A general solution of this equation has the fol-

lowing presentation

$$\omega(r, t) = \frac{\Gamma}{4\pi \left(\int_0^t \nu(\tau) d\tau + \sigma^2 \right)} \exp \left\{ -\frac{r^2}{4\pi \left(\int_0^t \nu(\tau) d\tau + \sigma^2 \right)} \right\}, \quad (40)$$

$$v(r, t) = \frac{1}{r} \int_0^r \omega(r', t) r' dr' = \frac{\Gamma}{2\pi r} \left(1 - \exp \left\{ -\frac{r^2}{4\pi \left(\int_0^t \nu(\tau) d\tau + \sigma^2 \right)} \right\} \right). \quad (41)$$

Here Γ is the integration constant having dimension m^2/s and σ is an arbitrary constant such that the denominator is always positive. The extra parameter σ emerges out of nowhere. But it provides supporting of vortex lifetime as long as possible.

If the viscosity does not depend on the time, i.e., $\nu = \text{const}$, this solution degenerates to the Lamb-Oseen solution [45], which decays with time. If $\nu(t)$ is an alternating function of time, at that on the average by time it stays equal to zero, then the vortex can live indefinitely. Let, for example, this function be as follows

$$\nu(t) = \nu \cos(\Omega t) = \nu \frac{e^{i\Omega t} + e^{-i\Omega t}}{2} \quad (42)$$

where Ω is an oscillation frequency and ϕ is an uncertain phase. Then the solution (40)-(41) looks as follows:

$$\omega(r, t) = \frac{\Gamma}{4\pi(\nu/\Omega)(\sin(\Omega t) + n)} \cdot \exp \left\{ -\frac{r^2}{4\pi(\nu/\Omega)(\sin(\Omega t) + n)} \right\}. \quad (43)$$

$$\vec{v}(r, t) = \frac{\Gamma}{2\pi r} \left(1 - \exp \left\{ -\frac{r^2}{4\pi(\nu/\Omega)(\sin(\Omega t) + n)} \right\} \right). \quad (44)$$

Here an arbitrary constant n should be greater than 1, and $(\nu/\Omega) \cdot n = \sigma^2$. These solutions

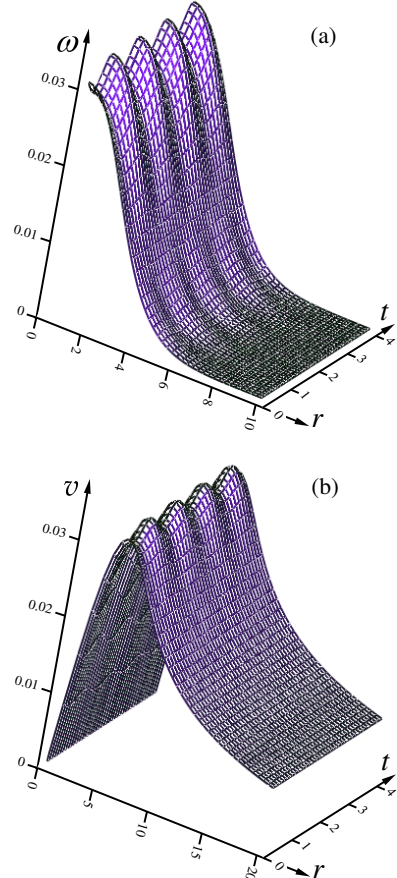


FIG. 2: Vorticity $\omega(r, t)$ in (a) and velocity $v(r, t)$ in (b) as functions of r and t for $\Gamma = 1$, $\nu = 1$, $\Omega = \pi$, and $n = 16$. These parameters are conditional with aim to show qualitative picture of oscillations of the vortex in time.

as functions of r and t are shown in Figs. 2(a) and 2(b), respectively. One can see that these functions undergo oscillations in the course of

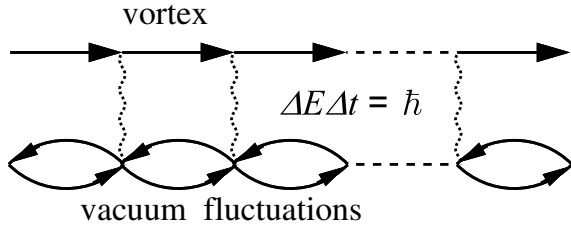


FIG. 3: Periodic energy exchange between the vortex and vacuum fluctuations

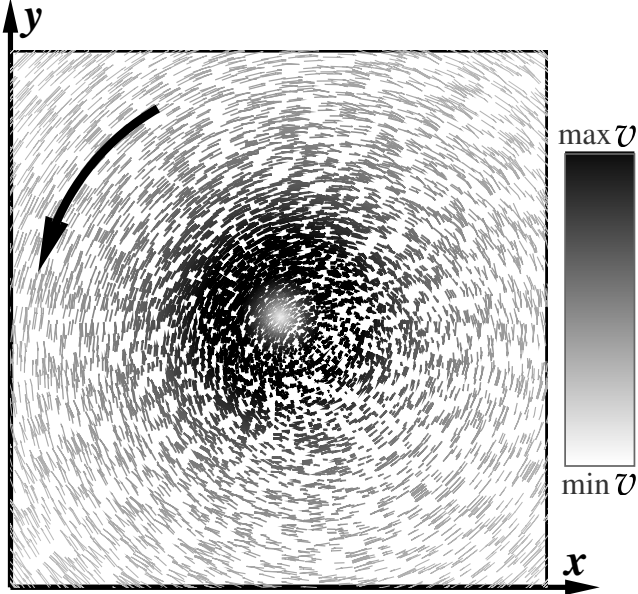


FIG. 4: Cross-section of the vortex tube in the plane (x, y) . Values of the velocity v are shown in grey ranging from light gray (min v) to dark grey (max v). Density of the pixels represents magnitude of the vorticity. Core of the vortex ω is well visible in the center.

time t . These functions do not attenuate with time, staying in the oscillating mode on all times.

The undamped solution was obtained thanks to assumption, that the kinematic viscosity is an alternating function of time. The viscosity is not a good term for the processes taking place in the quantum world. In that case the alternation of signs is considered as exchange of quantum energy of the vortex with vacuum states through the zero-point fluctuations, Fig 3. In the average, the viscosity of the fluid medium is equal to zero. It can mean that this medium is superfluid. Such a scenario is well known. At transition of helium to the superfluid phase [44], coherent Cooper pairs of electrons are formed by the exchange of phonons which play a role of fluctuations of a background medium.

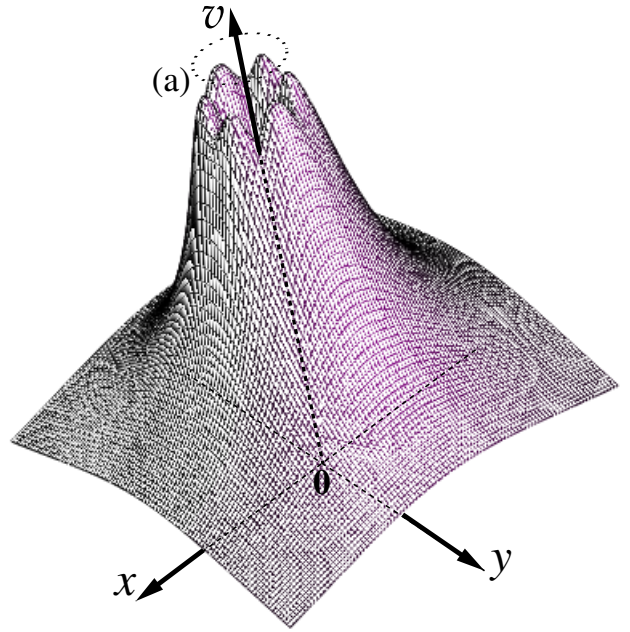


FIG. 5: Qualitative presentation of the vortex velocity v . Dotted circle (a) marks boundary of the wall of the core.

Qualitative view of the vortex tube in its cross-section is shown in Fig. 4. Values of the velocity v are shown by gray color ranging from light gray (min v) to dark gray (max v). In the center of the vortex, the vortex core (so-called "eye of the hurricane") is well viewed. Here it looks as a small light gray disk, where the velocities have small values. In the very center of the disk, in particular, the velocity vanishes. This is in stark contrast to conditions in the region where the strongest moving the medium occurs (in Fig. 4 it looks as a dark gray annular region enclosing the light gray inner area). This transition region is named the wall of the core. Fig. 5 shows a qualitative presentation of the vortex velocity. The wall of the core here is marked by the dotted circle (a). On this wall the velocity has wavy variations of its own values.

To evaluate the radius of the core we need to equate to zero the first derivative by r of Eq. (44) and to find its roots. Among two roots we find the root giving the interested radius [39]

$$r_{\text{core}} \approx 2\sqrt{a_0(n + \sin(\Omega t))} \sqrt{\frac{\nu}{\Omega}} \quad (45)$$

Here $a_0 \approx 1.2564$ is a root of the equation $\ln(2a_0 + 1) = a_0 = 0$. We see that the radius

is an oscillating function of time. The larger Ω , the more frequently these oscillations, i.e., the more quickly the vortex trembles. At that, as Ω increases, the core radius decreases. The radius grows with increasing n . However with $n \gg 1$ amplitude of these oscillations becomes negligibly small.

Let us evaluate the radius r_{core} by choosing the viscosity ν equal to $\hbar/2m$. In the case of electron mass, $m = 9.1 \cdot 10^{-31}$ kg, we have $\nu \approx 5.8 \cdot 10^{-5}$ m²/s. As for Ω , let it be equal to $2mc^2/\hbar$, or approximately $1.6 \cdot 10^{21}$ radians per second for electron. Here c is the speed of light. Then we have $(\nu/\Omega)^{1/2} \approx 1.93 \cdot 10^{-13}$ m. This length is seen to be smaller than the Compton wavelength, $\lambda_C = 2.426 \cdot 10^{-12}$ m, in about 12 times. So, for choosing $n \approx 31$ we find from Eq. (45) that the radius of the vortex is about the Compton wavelength. This number is quite enough to prevent any fatal catastrophe of the vortex. That is, the vortex is a long-lived robust object. From the above we see that, on a distance about the Compton wavelength, virtual particles can be involved into a vorticity dancing around the electron core, by polarizing the electron charge. This dancing happens at trembling motion of the electron with the frequency $\Omega = 2mc^2/\hbar$. That oscillating motion has a deep relation to the so-called "Zitterbewegung" [2, 19]

A. Vortex rings and vortex balls

If we roll up the vortex tube in a ring and glue together its opposite ends we obtain a vortex ring. Position of points on the helicoidal vortex ring [43] in the Cartesian coordinate system is given by the following set of equations

$$\begin{cases} x = (b_1 + a_0 \cos(\omega_0 t + \phi_0)) \cos(\omega_1 t + \phi_1), \\ y = (b_1 + a_0 \cos(\omega_0 t + \phi_0)) \sin(\omega_1 t + \phi_1), \\ z = a_0 \sin(\omega_0 t + \phi_0). \end{cases} \quad (46)$$

The helicoidal vortex ring, with the parameters $a_0 = 2$, $b_1 = 3$, $\omega_0 = 12\omega_1$, and $\phi_0 = \phi_1 = 0$, is drawn in Fig 6 by thick black spiral. It curls along the wall of the vortex, dyed here by light-gray color, as pointed by thick arrows.

The above equation parametrized by t creates

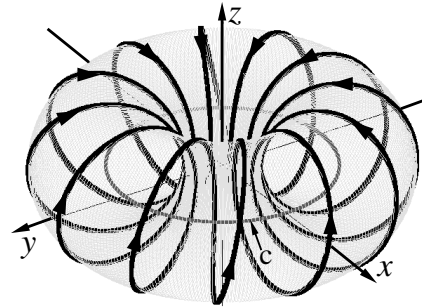


FIG. 6: Helicoidal vortex ring be drawn on the wall of the vortex core: $a_0 = 2$, $b_1 = 3$, $\omega_0 = 12\omega_1$, $\phi_0 = \phi_1 = 0$.

the helicoidal vortex ring. Parameters ω_0 and ω_1 are frequencies of rotation about the center of the tube on a course of thick arrows. Here a_0 is the radius of the tube curved along the circle pointed in the figure by arrow c . And b_1 is the distance from the center of the torus, located in the origin of coordinates (x, y, z) , to the center of the tube pointed by arrow c . A body of the tube, for the sake of visualization is colored in light-gray. The phases ϕ_0 and ϕ_1 have uncertain quantities ranging from 0 to 2π . By choosing the phases within this interval with a small increment, we may fill the torus by the helicoidal vortices everywhere densely.

Fig. 6 shows a qualitative view of the helicoidal vortex ring evolving on the wall of the vortex core. The vorticity here is maximal along the center of the tube. The velocity of revolution in the vicinity of this center is minimal. At the center it vanishes. However the velocity grows as a distance from the center increases. After reaching of some maximal value on the wall of the vortex core the velocity then begins to decrease.

1. The vortex balls

Instead the Hill's spherical vortex where all streamlines do not intersect, we shall consider vortex objects where intersections of the streamlines are allowed. These objects will be named the vortex balls. The name "vortex ball" originates from the fire-ball - an astonishing electromagnetic bundle of energy emerging often during thunderstorms.

While the radius b_1 is greater than a_0 the helical vortex ring will have a typical view as shown

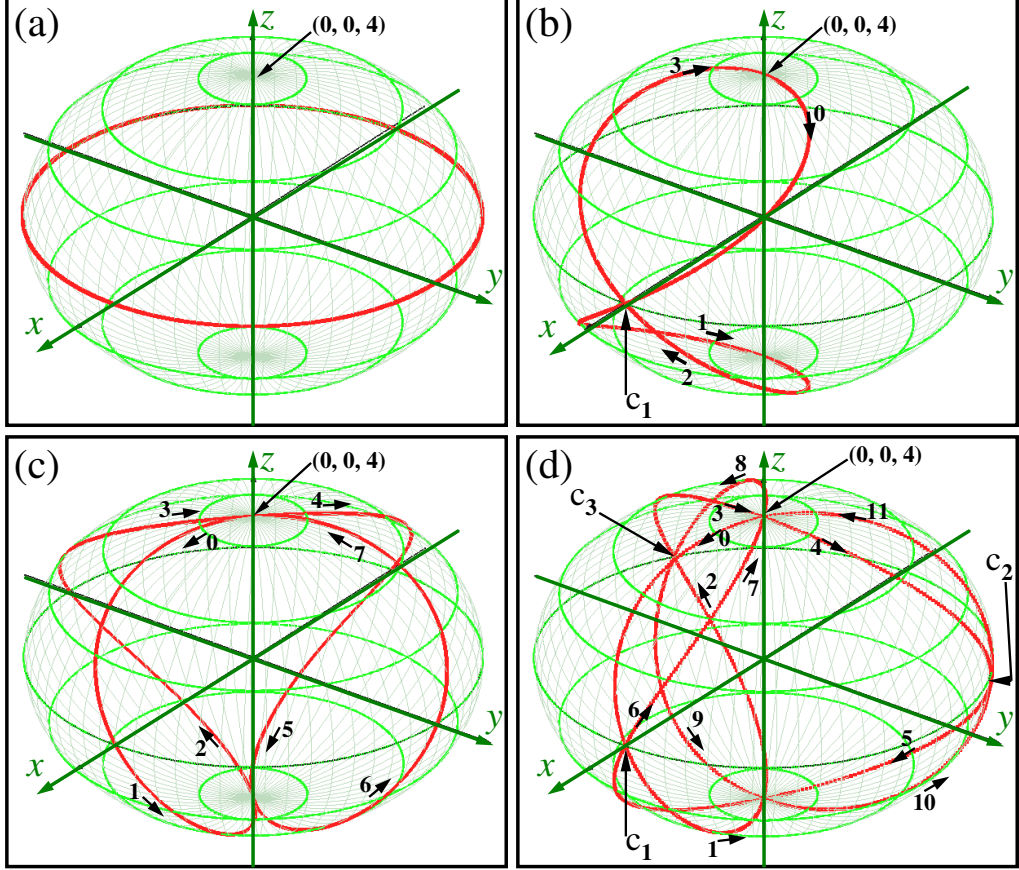


FIG. 7: Different modes of vortex rings having the radii $a_0 = 4$ and $b_1 = 0.01$, $(\phi_0 = \phi_1 = 0)$: (a) a degenerate loop, $\omega_0 = 0$ It lies in the plane (x, y) ; (b) single associated loop, $\omega_1 = \omega_0$; (c) double-associated loop, $\omega_1 = \omega_0/2$; (d) three times associated loop, $\omega_1 = \omega_0/3$. The arrows indicate the paths of travel along the loops. Thin circles emphasize the boundary of the vortex ball. Arrows c_1 , c_2 , and c_3 drawn in (b) and (d) point to intersections of the loops with themselves.

in Fig. 6. As soon as b_1 becomes smaller than a_0 the streamlines begin to intersect within the inner part of the helicoidal ring.

Let now the radius b_1 in Eq. (46) tends to zero. The helicoidal vortex ring in this case will transform into the vortex ring enveloping a spherical ball with the radius a_0 . Four different the vortex rings for the case of $a_0 = 4$, $b_1 \approx 0$ ($\phi_0 = \phi_1 = 0$) and for four different relationships of ω_0 to ω_1 drawn by thick curves are shown in Fig. 7.

The arrows 0, 1, 2, etc., indicate in Fig. 7 paths of the travel along the loops. One can see that except of the degenerate loop all loops begin from the point $(x, y, z) = (0, 0, 4)$ and after some time are returned in the same point. At that, the return to the top point for the single associated loop occurs through one revolution - through the revolution on 360 degrees, see Fig. 7(b). The return to the top point in the case

of the double-associated loop occurs through two revolutions, see Fig. 7(c). At the first revolution the arrow 0 changes its own orientation on opposite direction, see arrows 3 to 4. After the second revolution the arrow 7 acquires the initial orientation. So, the full revolution is $2 \cdot 360 = 720$ degrees. One can see that this motion is found in well agreement with the rotation of 1/2-spin. The return to the top point in the case of the three times associated loop occurs through three revolutions, see Fig. 7(d). So, the full revolution is equal to $3 \cdot 360 = 1080$ degrees. The full return to the top point, $(x, y, z) = (0, 0, 4)$, for the n -th associated loop can be achieved after the revolution on $n \cdot 360$ degrees.

Observe that in the case of odd n , the n -th associated loops cross their own paths at the points lying on the equatorial circle. In Figs. 7 (b) and (d) these points are pointed by arrows c_1 , c_2 ,

and c_3 . It would seem that such intersections of the streamlines will kill existence of the vortex balls. However the vortex balls tremble as time goes on (it was discussed above). It means that the streamlines tremble as well. Consequently, in these intersection points the trembling will permit to move through these obstacles. It is important to note that the same trembling provides conditions for rotation of the balls about the axis z as we shall see further.

2. The Calabi-Yau S^2 manifold and the spin-1/2 object

The Calabi-Yau manifolds play an important role in the modern string theory [47]. In order to see a simplest manifestation of the Calabi-Yau manifold in our task we draw the Calabi-Yau T^2 manifold shown in Fig. 8. Here T^2 is the torus of the dimension 2. This manifold has been drawn

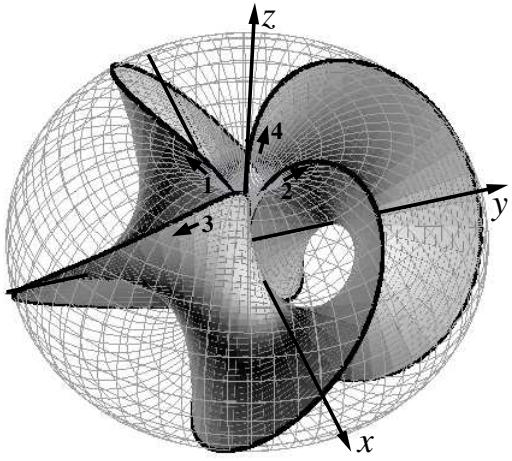


FIG. 8: Calabi-Yau T^2 manifold.

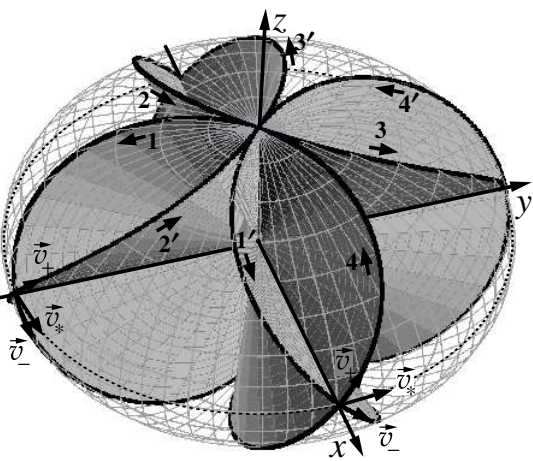


FIG. 9: Calabi-Yau S^2 manifold.

according to the formula (46) with the following set of the parameters: $\phi_0 = \phi_1 = 0$, $\omega_1 = \omega_0/2$, $b_1 = 1$, a_0 ranges from -1 to $+1$, and $\omega_0 t$ changes from 0 to 4π . Obviously for the sake of the strictness, we could use complex variables $\xi = x + iy$ and $\zeta = x - iy$. However this replacement is not critically for our low-dimensional tasks.

Two black curves in this Figure envelop the edges of the manifold. The first curve (for $b_1 = 1$, $a_0 = 1$, $\phi_0 = 0$, and $\phi_1 = 0$) is marked by arrows going from 1 to 2. The second curve (for $b_1 = 1$, $a_0 = 1$, $\phi_0 = 0$, and $\phi_1 = \pi/2$) is marked by arrow going from 3 to 4. These curves lie on the surface of the torus, which is drawn by light grey lines. Observe that all arrows in Fig. 8 come out of the center of the torus upwards along the black curves lying on the surface of the torus.

Topological transformation can be fulfilled through the parameter b_1 tending to zero. In this case the Calabi-Yau T^2 manifold transforms to the Calabi-Yau S^2 manifold shown in Fig. 9. One can see that this manifold is embedded in the sphere S^2 which is drawn by light-gray lines. The two double-associated loops drawn by black thick curves envelop the manifold along its edges. These loops shifted with respect to each other on the phase $\phi_1 = \pi/2$ lie on the surface of the sphere. The first loop (the phase is $\phi_1 = 0$) bypasses the path along the arrows 1 to 2 to 3 to 4 and further again to 1. And the second loop (the phase is $\phi_1 = \pi/2$) bypasses the path along the arrows 1' to 2' to 3' to 4' and further again to 1'. Observe that the paths pass through the pole localized in the point $z = \pm 1$ always in opposite directions. It means that the path can pass the pole in the same direction only after the repeated traversal of the path, see Fig. 7(c) for more details.

One can see that the loops in Fig. 9 intersect with each other on the equatorial circle drawn by dotted curve. Let us imagine that a small clot moves along the loop. The motion of the elementary clots along the vortex loops takes place with the velocity

$$\vec{v}_R = \begin{cases} v_x = -a_0\omega_0 \sin(\omega_0 t + \phi_0) \cos(\omega_1 t + \phi_1) - a_0\omega_1 \cos(\omega_0 t + \phi_0) \sin(\omega_1 t + \phi_1) \\ \quad - b_1\omega_1 \sin(\omega_1 t + \phi_1), \\ v_y = -a_0\omega_0 \sin(\omega_0 t + \phi_0) \sin(\omega_1 t + \phi_1) + a_0\omega_1 \cos(\omega_0 t + \phi_0) \cos(\omega_1 t + \phi_1) \\ \quad + b_1\omega_1 \cos(\omega_1 t + \phi_1), \\ v_z = a_0\omega_0 \cos(\omega_0 t + \phi_0), \end{cases} \quad (47)$$

Four intersection points lying on the equatorial circle are points where superpositions of the velocities \vec{v}_+ and \vec{v}_- give the summary velocity \vec{v}_* oriented along the equatorial circle. Two such intersection points can be seen in foreground in Fig. 9. One can see that the total motion along the equatorial circle takes place about the axis z counter-clockwise, if we look from the top. Here we write the subscripts $+$, $-$, and $*$ instead of R in order to emphasize orientations of the velocities on the Calabi–Yau S^2 manifold.

In the vicinity of the intersection points the velocities \vec{v}_+ and \vec{v}_- are calculated according to Eq. (47) with the parameters $a_0 = 1$, $b_1 = 0.01$, and $\omega_1 = \omega_0/2$. The first velocity is calculated with the phases $\phi_0 = 0$, $\phi_1 = 0$, and the second is calculated with the phases $\phi_0 = 0$, $\phi_1 = \pi/2$. Infinitesimal shifts along these streamlines give new locations on them:

$$\vec{r}_\pm = \vec{r}_0 + \vec{v}_\pm \delta t. \quad (48)$$

Here \vec{r}_0 is a position of the intersection point either in the first knot or in the second knot. And δt represents the infinitesimal time shift. The new position

$$\vec{r}_* = \vec{r}_+ + \vec{r}_- = \vec{r}_0 + \vec{v}_* \delta t \quad (49)$$

lies on the circle, whose plane is perpendicular to the axis z . Here $\vec{v}_* = \vec{v}_+ + \vec{v}_-$ has non-zero components $v_x \delta t$ and $v_y \delta t$ whereas $v_z \delta t$ is equal to zero. It means that the motion occurs about the axis z in the plane perpendicular to it.

By choosing the loops with other phases ϕ_0 and ϕ_1 one can cover the surface of the sphere S^2 by the intersection points everywhere densely. In these points the sum of the velocities \vec{v}_+ and \vec{v}_- gives the summary velocity \vec{v}_* lying in the plane (x, y) . All these velocities are oriented in the same direction about the axis z . So that, the

resulting rotation will occur about the axis z , as shown in Fig. 10.

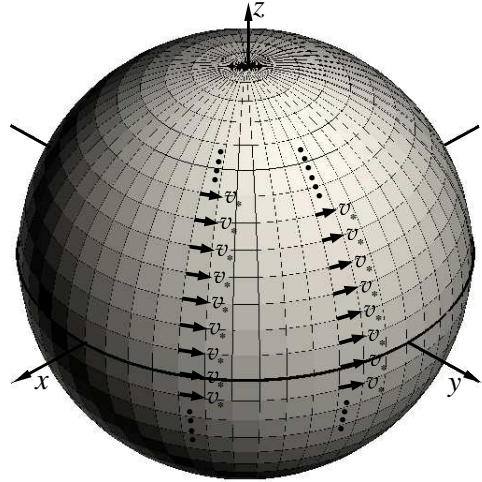


FIG. 10: Qualitative presentation of the self-organizing flow on the wall of the vortex core: $a_0 = 4$, $b_1 = 0.01$.

It would seem that the sum of two shifts, $\vec{v}_+ \delta t$ and $\vec{v}_- \delta t$, leads to an uncertain total shift, as follows from the uncertainty principle. However we need to take in account that superposition of many flows on the vortex ball reduces to constructive and destructive interference pattern on it. All they provide the total shifts oriented in the same direction. In the whole, a self-organized flow about the axis z arises Fig. 10.

It should be noted that this self-organizing flow rotating about the axis z repeats itself after each revolution on 720 degrees. Figurally speaking, the vortex ball changes its color through each revolution on 360 degrees, say, green, red, green, red, and so forth. In the quaternion representation we may imagine themselves [1] that a tip of the spin rotates on surface of 3D sphere. After the revolution of the spin on 360 degrees, a flag attached to the tip (let it be the harpoon-arrow, for example) turns only on 180 degrees.

Let us look on these transformations with the

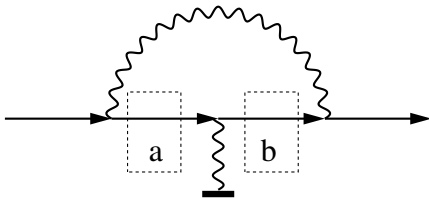


FIG. 11: The Feynman diagram showing the lowest-order (second-order) contribution to the anomalous magnetic moment. Rectangles a and b drawn by dotted lines highlight areas where the similar second-order diagrams can be realized. Thick line drawn below the wavy line marks the zero-point vacuum background (as a symbol of the ground in electronic circuit diagrams).

perspective of the group $SU(2)$. First we define the angular velocity, $\vec{\Omega}$, as the rate of change of angular displacement of the flag (the harpoon-arrow) on the sphere with the radius a_0 :

$$\vec{\Omega} = \frac{\vec{r} \times \vec{v}_R}{|r|^2} \Big|_{r=a_0} \quad (50)$$

Now we rewrite Eq. (47) in assumption $b_1 \rightarrow 0$, $\omega_1 = \omega_0/2$ (hereinafter, for the sake of simplicity, we shall omit subscript 0), and let the phases, ϕ_0 and ϕ_1 , be absent. We have:

$$\begin{aligned} \Omega_+ &= \Omega_x + i\Omega_y \\ &= -\frac{1}{2}\omega \exp\left\{i\frac{\omega}{2}t\right\} (2\sin(\omega t) - i\cos(\omega t)), \\ \Omega_- &= \Omega_x - i\Omega_y \\ &= -\frac{1}{2}\omega \exp\left\{-i\frac{\omega}{2}t\right\} (2\sin(\omega t) + i\cos(\omega t)), \\ \Omega_z &= \omega \cos(\omega t). \end{aligned} \quad (51)$$

Here $\Omega_x = v_x/a_0$, $\Omega_y = v_y/a_0$, $\Omega_z = v_z/a_0$.

Now we may write an equation describing behavior of the spin-1/2 under the influence of a field $(\hbar\Omega_x, \hbar\Omega_y, \hbar\Omega_z)$ [34]

$$i\hbar \frac{\partial}{\partial t} \begin{pmatrix} \psi_\uparrow \\ \psi_\downarrow \end{pmatrix} = \begin{pmatrix} \theta_z & \theta_x - i\theta_y \\ \theta_x + i\theta_y & -\theta_z \end{pmatrix} \begin{pmatrix} \psi_\uparrow \\ \psi_\downarrow \end{pmatrix}. \quad (52)$$

Here the energy coefficients $(\theta_x, \theta_y, \theta_z)$ stem from $(\Omega_x, \Omega_y, \Omega_z)$ by multiplying the latter by \hbar . More definitely $\hbar\omega$ represents the energy level of the rotation about axis z .

We may continue this consideration by introducing the magnetic field \vec{B} [31] that acts on

the spin-1/2 particle in the following manner $\vec{\theta} = \mu_e(\vec{\sigma}, \vec{B})$. Here $\vec{\sigma}$ is the 3-component operator consisting of 2×2 Pauli matrices σ_x , σ_y , and σ_z . Let μ_e be in the first approximation, the Bohr magneton

$$\mu_B = \frac{e\hbar}{2m_e} \approx -9.27401452557 \times 10^{-24} \text{ J} \cdot \text{T}^{-1}, \quad (53)$$

which gives the magnetic moment of the Dirac electron. Here e is the electron charge (it is negative) and m_e is its mass. System of units adopted here is SI.

Observe, however, that the electron has the anomalous magnetic moment that slightly differs from the above value. This difference is induced by interaction of the charged particle with the zero-point oscillations of the electromagnetic field [30]. Really, this interaction is due to exchange of the particle energy with the vacuum zero-point oscillations. In our case, it is exhibited in that the vortex draws into a whirl the vacuum fluctuations far away of the vortex core. These whirling dances fluctuate about some averaged level because of exchanging the energy with the zero-point vacuum background.

Schwinger was first who can calculate in 1947 the anomalous magnetic moment [41] in a good agreement with the experiment

$$\begin{aligned} \mu_e &= \mu_B (1 + \alpha/2\pi) \\ &\approx -9.28478137856 \times 10^{-24} \text{ J} \cdot \text{T}^{-1}. \end{aligned} \quad (54)$$

He has applied the one-loop correction for calculation of the anomalous magnetic moment as shown in Fig 11. Here $\alpha = e^2/(4\pi\epsilon_0\hbar c)$ is the fine structure constant, ϵ_0 is the vacuum permittivity, and c is the light velocity.

In fact, Schwinger has shown, that the fine structure constant (namely, the term $\alpha/2\pi$) plays an important role at calculating the anomalous magnetic moment. Sommerfeld in 1958 has calculated a more exact value of the anomalous magnetic moment [42]

$$\begin{aligned} \mu_e &\approx \mu_B (1 + \alpha/2\pi - 1.312(\alpha/2\pi)^2) \\ &= -9.284764966 \times 10^{-24} \text{ J} \cdot \text{T}^{-1}. \end{aligned} \quad (55)$$

For comparison, the most accurate value for the electron magnetic moment is as follows $\mu_e = (-9.28476377 \pm 0.00000023) \times 10^{-24} \text{ J} \cdot \text{T}^{-1}$.

We may guess that the term $\alpha/2\pi$ can manifest itself through a fractal cascade of the second-order diagrams. One may highlight areas where the similar diagrams can be realized. See rectangles drawn by dotted lines in Fig 11. A contri-

bution of the second-order diagram falls with its positions on more deep level. However amount of these diagrams grows as $n!$. It gives a hint, that such a fractal diagram can be reproduced as the continued fraction:

$$\mu_e = \mu_B \frac{1}{1 - \frac{1}{1 + \dots}}}}}}}}}}. \quad (56)$$

Note that signs in this fraction alternate as follows $-,-,+,-,-,+,\dots$, the Bohr magneton has negative sign, see Eq. (53). The calculation of this fraction up to the contribution of the member $1 - 18! \alpha/2\pi$ gives the following result $\mu_e \approx -9.28476339 \times 10^{-24} \text{ J} \cdot \text{T}^{-1}$. Observe that if we restrict themselves at calculation of the fraction by the member $1 - 6! \alpha/2\pi$ we get $\mu_e \approx -9.28476377 \times 10^{-24} \text{ J} \cdot \text{T}^{-1}$.

V. CONCLUSION

The Navier-Stokes equation supplemented by the two slightly modified terms represents a basic equation underlying the non-relativistic Schrödinger equation. These two modifications concern the inner forces that take place within a fluid medium under consideration. The first force is the gradient pressure supplemented by the gradient of the quantum entropy multiplied by the pressure. It turns out that such a modification induces emergence of the quantum potential. The second force is a dissipative force con-

ditioned by viscosity of the fluid medium. The modification of this term is that we admit that the viscosity in the average of the time vanishes, but its variance is not zero. Factually, the viscosity changes its own sign with the time. It means that there is an energy exchange within this medium. For that reason the fluid medium represents itself as the superfluid vacuum consisting of enormous amount of virtual particle-antiparticle pairs. Really, the superfluid vacuum is represented as the Bose-Einstein condensate.

Induced in this medium the vortices can live indefinitely long. The vortex has a core where the velocity of rotation tends to zero in the center of the core. On the other hand, on the wall of the core the velocity reaches a maximal value. Then, it falls to zero on infinity.

An important observation is that the vortex experiences the trembling because of the viscosity fluctuating about zero. This trembling is akin to so-called "Zitterbewegung" - a rapid motion of elementary particles, in particular electrons, described by the Dirac equation [2, 19]. In our

case the trembling is caused by regular energy exchange of the vortex with the zero-point fluctuations of the vacuum. Our observations say that this trembling provides an infinite lifetime of the vortices.

The vortex rolled up in a ring and transformed further into a spherical bubble, named the vortex ball by analogy with the light ball, gives an image of the particle. The latter moves along an optimal path stemming from solution of the Schrodinger equation. In fact, these optimal paths are the Bohmian trajectories. A motion along such a trajectory is not really observable, since the observation faces with the uncertainty principle. This principle forbids the simultaneous measurement of two complementary variables, as for example of the momentum of the particle and its coordinate. Nevertheless, the particle continues to move along the optimal path, the Bohmian trajectory, until it is perturbed.

Observe that the global circulation on the wall of the vortex core occurs along a complex trajectory. The full revolution can be reached after ro-

tation on 360 degrees, or $720 = 2 \cdot 360$ degrees, or $1080 = 3 \cdot 360$ degrees, and so forth. One can see that the full revolution on 720 degrees is typical for behavior of the particle with the spin 1/2. So, the vortex balls can simulate the spin 1/2 particle.

The Navier-Stokes equation loaded by two slight modifications contains a rich set of solutions. First, the equation gives description of an amazing superfluid medium, the physical vacuum. Apart of it, this equation contains solutions of vortices. The vortex once arising can live infinitely long. In the course of its evolution, the vortex performs trembling motions.

Acknowledgments

The author thanks Mike Cavedon and Pat Noland for useful and valuable remarks and offers. The author thanks also Miss Pipa (Quantum Portal administrator) for preparing a program drawing Fig. 1.

[1] M. M. Agamalyan, G. M. Drabkin, and V. I. Sbitnev. Spatial spin resonance of polarized neutrons. A tunable slow neutron filter. *Physics Reports*, 168(5):265–303, 1988. doi:10.1016/0370-1573(88)90081-6.

[2] A. O. Barut and A. J. Bracken. *Zitterbewegung and the internal geometry of the electron*. *Phys. Rev. D*, 23(10): 2454–2463, 1981. doi:10.1103/PhysRevD.23.2454.

[3] A. Benseñy, G. Albareda, A. S. Sanz, J. Mompart, and X. Oriols. Applied Bohmian mechanics. *Eur. Phys. J. D*, 68:286–328, 2014. doi:10.1140/epjd/e2014-50222-4.

[4] M. V. Berry, R. G. Chambers, M. D. Large, C. Upstill, and J. C. Walmsley. Wavefront dislocations in the Aharonov-Bohm effect and its water wave analogue. *European Journal of Physics*, 1(3):154–162, 1980. doi:10.1088/0143-0807/1/3/008.

[5] D. Bohm. A suggested interpretation of the quantum theory in terms of "hidden" variables. I. *Phys. Rev.*, 85 (2):166–179, 1952. doi:10.1103/PhysRev.85.166.

[6] D. Bohm. A suggested interpretation of the quantum theory in terms of "hidden" variables. II. *Phys. Rev.*, 85 (2):180–193, 1952. doi:10.1103/PhysRev.85.180.

[7] D. Bohm and J. P. Vigier. Model of the causal interpretation of quantum theory in terms of a fluid with irregular fluctuations. *Phys. Rev.*, 96:208–216, 1954. doi:10.1103/PhysRev.96.208.

[8] C. Gh. Buzea, M. Agop, and C. Nejneru. Correspondences of scale relativity theory with quantum mechanics. In M. R. Pahlavani, editor, *Theoretical concept of Quantum Mechanics*, chapter 18, pages 409–444. InTech, Rijeka, 2012. doi:10.5772/34259.

[9] Y. Couder and E. Fort. Single-particle diffraction and interference at a macroscopic scale. *Phys. Rev. Lett.*, 97: 154101, 2006. doi:10.1103/PhysRevLett.97.154101.

[10] P. D. Damázio and R. A. Siqueira. Strong solutions of Navier-Stokes equations of quantum incompressible fluids, (8 Feb 2013). URL <http://people.ufpr.br/~pddamazio/quantum-fluids-Damazio-Siqueira.pdf>.

[11] L. de Broglie. Interpretation of quantum mechanics by the double solution theory. *Annales de la Fondation Louis de Broglie*, 12(4):1–22, 1987.

[12] D. Derbes. Feynman's derivation of the schrödinger equation. *Am. J. Phys.*, 64(7):881–884, 1996.

[13] R. J. Donnelly. *Quantized Vortices in Helium II*. Cambridge UniversityPress, Cambridge, NY, 1991.

[14] A. Eddi, E. Sultan, J. Moukhtar, E. Fort, and Y. Rossi, M. and. Couder. Information stored in faraday waves: the origin of a path memory. *J. Fluid Mech.*, 674:433–463, 2011. doi:10.1017/S0022112011000176.

[15] R. P. Feynman and A. Hibbs. *Quantum Mechanics and Path Integrals*. McGraw Hill, N. Y., 1965.

[16] G. Grössing. Sub-quantum thermodynamics as a basis of emergent quantum mechanics. *Entropy*, 12:1975–2044, 2010. doi:10.3390/e12091975.

[17] J. B. . Hartle. What connects different interpretations of quantum mechanics? In Elitzur A., Dolev S., and Kolenda N., editor, *Quo Vadis Quantum Mechanics?*,

pages 72–82. Springer, Berlin, Heidelberg, New York, 2005.

[18] R. J. Harvey. Navier-Stokes analog of quantum mechanics. *Phys. Rev.*, 152:1115, 1966. doi:10.1103/PhysRev.152.1115.

[19] D. Hestenes. The zitterbewegung interpretation of quantum mechanics. *Found. Physics.*, 20(10):1213–1232, 1990. doi:10.1007/BF01889466.

[20] P. Holland. Hydrodynamic construction of the electromagnetic field. *Proc. R. Soc. A*, 461:3659–3679, 2005. doi:10.1098/rspa.2005.1525.

[21] R. Jackiw, V. P. Nair, S.-Y. Pi, and A. P. Polychronakos. Perfect fluid theory and its extensions. *J. Phys. A*, 37:R327–R432, 2004. URL <http://arxiv.org/abs/hep-ph/0407101>.

[22] T. Juffmann, S. Truppe, P. Geyer, A. G. Major, S. Deachapunya, H. Ulbricht, and M. Arndt. Wave and particle in molecular interference lithography. *Phys. Rev. Lett.*, 103:263601, 2009. doi:10.1103/PhysRevLett.103.263601.

[23] A. Jüngel and J-P. Milišić. Quantum Navier-Stokes equations. Progress in industrial. *Mathematics at ECMI 2010. Mathematics in Industry.*, 17:427–439, 2012.

[24] P. Kundu and I. Cohen. *Fluid Mechanics*. Academic Press, 2002.

[25] L. D. Landau and E. M. Lifshitz. *Fluid mechanics*. Pergamon Press, Oxford, 1987.

[26] I. Licata and D. Fiscaletti. Bell length as mutual information in quantum interference. *Axioms*, 3(2):153–165, 2014. doi:10.3390/axioms3020153.

[27] I. Licata and D. Fiscaletti. *Quantum potential: Physics, Geometry, and Algebra*. Springer, Cham, Heidelberg, N. Y., Dordrecht, London, 2014.

[28] E. Madelung. Quantumtheorie in hydrodynamische form. *Zts. f. Phys.*, 40:322–326, 1926.

[29] N. Makri. Feynman path integration in quantum dynamics. *Computer Physics Communications*, 63:389–414, 1991.

[30] N. B. Mandache. On the physical origin of the anomalous magnetic moment of electron, 1307.2063, (8 Jul 2013). URL <http://arxiv.org/abs/1307.2063>.

[31] A. A. Martins. Fluidic electrodynamics: On parallels between electromagnetic and fluidic inertia, 1202.4611, (21 Feb 2012). URL <http://arxiv.org/abs/1202.4611>.

[32] E. Nelson. Derivation of the Schrödinger equation from Newtonian mechanics. *Phys. Rev.*, 150:1079–1085, 1966. doi:10.1103/PhysRev.150.1079.

[33] S. Protieré, A. Boudaoud, and Y. Couder. Particle-wave association on a fluid interface. *J. Fluid Mech.*, 554:85–108, 2006. doi:10.1017/S0022112006009190.

[34] V. I. Sbitnev. Spinning particle in a magnetic field - the Pauli equation and its splitting into two equations for real functions. *Quantum Magic*, 5(2):2112–2131, 2008. URL <http://quantmagic.narod.ru/volumes/VOL522008/p2112.html>.

[35] V. I. Sbitnev. Bohmian trajectories and the path integral paradigm: complexified Lagrangian mechanics. *Int. J. Bifurcation & Chaos*, 19(7):2335–2346, 2009. doi:10.1142/S0218127409024104.

[36] V. I. Sbitnev. Bohmian trajectories and the path integral paradigm - complexified Lagrangian mechanics. In Pahlavani, M. R., editor, *Theoretical Concepts of Quantum Mechanics*, chapter 15, pages 313–334. InTech, Rijeka, 2012. doi:10.5772/33064.

[37] V. I. Sbitnev. Generalized path integral technique: nanoparticles incident on a slit grating, matter wave interference. In Bracken, P., editor, *Advances in Quantum Mechanics*, chapter 9, pages 183–211. InTech, Rijeka, 2013. doi:10.5772/53471.

[38] V. I. Sbitnev. From the Newton's laws to motions of the fluid and superfluid vacuum: vortex tubes, rings, and others, 1403.3900, (20 Jun 2014). URL <http://arxiv.org/abs/1403.3900>.

[39] V. I. Sbitnev. Physical vacuum is a special superfluid medium. In Pahlavani, M. R., editor, *Quantum Mechanics*. InTech, Rijeka, 2014.

[40] E. Schrödinger. An undulatory theory of the mechanics of atoms and molecules. *Phys. Rev.*, 28(6):1049–1070, 1926.

[41] J. Schwinger. On quantum-electrodynamics and the magnetic moment of the electron. *Phys. Rev.*, 73:416–418, 1948. doi:10.1103/PhysRev.73.416.

[42] Ch. M. Sommerfield. The magnetic moment of the electron. *Annals of Physics*, 5(1):26–57, 1958. doi:10.1016/0003-4916(58)90003-4.

[43] E. B. Sonin. Dynamics of helical vortices and helical-vortex rings. *Europhys. Lett.*, 97:46002, 2012. doi:10.1209/0295-5075/97/46002.

[44] G. E. Volovik. *The Universe in a Helium Droplet*. Oxford University Press, Oxford, 2003.

[45] Wu Jie-Zhi, Ma Hui-Yang, and Zhou Ming-De. *Vorticity and Vortex Dynamics*. Springer-Verlag, Berlin Heidelberg, 2006.

[46] R. E. Wyatt. *Quantum dynamics with trajectories: Introduction to quantum hydrodynamics*. Springer, N. Y., 2005.

[47] S.-T Yau and S. Nadis. *The shape of inner space. String theory and the geometry of the Universe's hidden dimensions*. Basic Books, N. Y., 2010.